1521-0111/94/6/1371–1381$35.00
MOLECULAR PHARMACOLOGY

https://doi.org/10.1124/mol.118.113373
Mol Pharmacol 94:1371–1381, December 2018

Homogeneous, Real-Time NanoBRET Binding Assays for the Histamine H_3 and H_4 Receptors on Living Cells[S]

Tamara A. M. Mocking, Eléonore W. E. Verweij, Henry F. Vischer, and Rob Leurs

Amsterdam Institute for Molecules, Medicines and Systems, Division of Medicinal Chemistry, Faculty of Science, Vrije Universiteit Amsterdam, Amsterdam, The Netherlands

Received June 13, 2018; accepted September 19, 2018

ABSTRACT

Receptor-binding affinity and ligand-receptor residence time are key parameters for the selection of drug candidates and are routinely determined using radioligand competition-binding assays. Recently, a novel bioluminescence resonance energy transfer (BRET) method utilizing a NanoLuc-fused receptor was introduced to detect fluorescent ligand binding. Moreover, this NanoBRET method gives the opportunity to follow fluorescent ligand binding on intact cells in real time, and therefore, results might better reflect in vivo conditions as compared with the routinely used cell homogenates or purified membrane fractions. In this study, a real-time NanoBRET-based binding assay was established and validated to detect binding of unlabeled ligands to the histamine H_3 receptor (H_3R) and histamine H_4 receptor on intact cells. Obtained residence times of clinically tested H_3R antagonists were reflected by their duration of H_3R antagonism in a functional receptor recovery assay.

Introduction

Blockbuster antihistamines targeting the histamine H_1 and H_2 receptors have been used for many decades to alleviate allergy symptoms and gastric acid–related disorders, respectively (Panula et al., 2015). In contrast, drug discovery programs on the other two members of the histamine receptor family are still ongoing. The histamine H_3 receptor (H_3R) is predominantly expressed in the central nervous system and considered a therapeutic target for neurologic disorders, such as Alzheimer's and Parkinson's diseases, attention deficit hyperactivity disorder, epilepsy, and narcolepsy (Wijtmans et al., 2007; Sadek et al., 2016). The histamine H_4 receptor (H_4R) is predominantly expressed on immune cells and linked to inflammatory disorders, such as psoriasis, atopic dermatitis, asthma, and arthritis (Novak et al., 2012; Verweij et al., 2017). In 2016, the first H_3R-targeting therapeutic, pitolisant (Wakix, Bioprojet Pharma, Paris, France), was approved by the European Medicine Agency for the treatment of narcolepsy (Kollb-Sielecka et al., 2017), whereas H_4R-targeting drug candidates are in clinical trials for the treatment of various inflammatory disorders (Thurmond, 2015; Attali et al., 2016; Thurmond et al., 2017).

Traditionally, radioligands are used in competition binding experiments to indirectly determine the binding affinities (K_i), association (k_{on}), and dissociation (k_{off}) rate constants of the binding of unlabeled ligands to a receptor. However, these radioligand-based methods generally require physical separation of free and bound radioligands to quantify receptor-bound radioligand. Consequently, these endpoint assays are particularly labor intensive, as each measured time point requires a separate binding reaction. Recently, a novel proximity-based method was introduced for the histamine H_1 receptor and a number of other G protein–coupled receptors (GPCRs) by genetic fusion of an engineered enzyme, NanoLuc (Nluc), to the N-terminus of these receptors, allowing only the detection of bound fluorescent ligand via bioluminescence resonance energy transfer (nanoBRET). Consequently, this novel method does not require physical separation of free from bound fluorescent ligand (Stoddart et al., 2015; Soave et al., 2016). Hence, this proximity-based (<10 nm) method allows real-time measurement of ligand binding to GPCRs on intact cells. Moreover, no additional prelabeling steps are required in contrast to the

This work was supported by The Netherlands Organization for Scientific Research (NWO) TOPPUNT ["7 ways to 7TMR modulation (7-to-7)"] [Grant 718.014.002] and ECHO [Grant 711.013.014].
https://doi.org/10.1124/mol.118.113373.
[S] This article has supplemental material available at molpharm.aspetjournals.org.

ABBREVIATIONS: A-331440, (4′-[3-(3(R)-(dimethylamino)-pyrrolidin-1-yl)-propoxy]-biphenyl-4-carbonitrile; A-349821, ([4′-{3-([R,R]2,5-dimethyl-pyrrolidin-1-yl)-propoxy}-biphenyl-4-yl]-morpholin-4-yl-methanone; ABT-239, 4-(2-{2-[(2R)-2-Methylpyrrolidin-1-yl]ethyl}-benzofuran-5-yl)benzonitrile; BRET, bioluminescence resonance energy transfer; CAMYEL, cAMP sensor using YFP-Epac-RLuc; clo-BDY, clobenpropit-BODIPY; CRE, cAMP-responsive element; FL-histamine, BODIPY-FL-histamine; GPCR, G protein–coupled receptor; GSK1004723, 4-[(4-Chlorophenyl)methyl]-2-({(2*R*)-1-[4-(4-{[3-(hexahydro-1*H*-azepin-1-yl)propyl]oxy}phenyl)butyl]-2-pyrrolidinyl}methyl)-1(2*H*)-phthalazinone; GSK189254, 6-[(3-cyclobutyl-2,3,4,5-tetrahydro-1H-3-benzazepin-7-yl)oxy]-N-methylpyridine-3-carboxamide; HBSS, Hanks' balanced salt solution; HEK293T, human embryonic kidney 293T; hH_3R, human H_3R; hH_4R, human H_4R; H_3R, histamine H_3 receptor, H_4R, histamine H_4 receptor; JNJ31001074, (4-Cyclopropyl-piperazin-1-yl)-(4-morpholin-4-ylmethyl-phenyl)-methanone, A-331440: (4′-[3-(3(*R*)-(dimethylamino)-pyrrolidin-1-yl)-propoxy]-biphenyl-4-carbonitrile; JNJ7777120, 1-[(5-chloro-1*H*-indol-2-yl) carbonyl]-4-methylpiperazine; NAMH, N^{α}-methylhistamine; [^{3}H]NAMH, N^{α}-[*methyl*-^{3}H]histamine [^{3}H]; Nluc, NanoLuc luciferase; PBS, phosphate-buffered saline; PEI, polyethyleneimine; PF-03654746, Trans-N-Ethyl-3-fluoro-3-[3-fluoro-4-(1-pyrrolidinylmethyl)phenyl]-cyclobutanecarboxamide 4-methylbenzenesulfonate; RT, residence time; SAMH, s-α-methylhistamine.

time-resolved fluorescence resonance energy transfer–based Tag-lite ligand-receptor-binding assay, which uses Tb^{3+}-cryptate conjugated to an N-terminal SNAP-tagged receptor as a resonance energy transfer donor (Zwier et al., 2010; Sykes et al., 2017). The development and commercial availability of fluorescent H_3R and H_4R ligands urged us to set up and validate a NanoBRET-based binding assay for the H_3R and H_4R (Tomasch et al., 2012; Vernall et al., 2014; Mirzahosseini et al., 2015). In this study, a NanoBRET-based binding assay was established and validated to detect binding of unlabeled ligands to the human H_3R (hH_3R) and human H_4R (hH_4R) on intact cells.

Materials and Methods

Materials. N^{α}-[*methyl*-^{3}H]histamine ([^{3}H]NAMH) (specific activity 79.7 Ci/mmol), [^{3}H]histamine (specific activity 10.6 Ci/mmol), Microscint-O scintillation liquid, and GF/C filter plates were purchased from PerkinElmer (Groningen, The Netherlands). Clobenpropit-BODIPY-630/650 (clo-BDY, CA200843) was purchased from Hello Bio (Bristol, UK), and BODIPY-FL-histamine (FL-histamine) was purchased from Setareh Biotech (Eugene, OR). Thioperamide and clobenpropit were purchased from Abcam (Cambridge, UK), Trans-N-Ethyl-3-fluoro-3-[3-fluoro-4-(1-pyrrolidinylmethyl)phenyl]-cyclobutanecarboxamide 4-methylbenzenesulfonate (PF-03654746) and 4-(2-{2-[(2R)-2-Methylpyrrolidin-1-yl]ethyl}-benzofuran-5-yl)benzonitrile (ABT-239) were obtained from Axon Medchem (Groningen, The Netherlands), and *S*-α-methylhistamine (SAMH) and N^{α}-methylhistamine (NAMH) were obtained from Tocris (Abingdon, UK). Pitolisant and (4-Cyclopropyl-piperazin-1-yl)-(4-morpholin-4-ylmethyl-phenyl)-methanone bavisant (JNJ31001074) were obtained from Griffin Discoveries (Amsterdam, The Netherlands). A-331440 [(4′-[3-(3(R)-(dimethylamino)-pyrrolidin-1-yl)-propoxy]-biphenyl-4-carbonitrile] was synthesized at the Department of Radiology and Nuclear Medicine, VU University Medical Center Amsterdam (Amsterdam, The Netherlands) and is commercially available at Tocris. GSK1004723 (4-[(4-Chlorophenyl)methyl]-2-({(2*R*)-1-[4-(4-{[3-(hexahydro-1*H*-azepin-1-yl)propyl]oxy}phenyl)butyl]-2-pyrrolidinyl}methyl)-1(2*H*)-phthalazinone) was a kind gift from Dr. Slack from GlaxoSmithKline (Stevenage, UK) (Slack et al., 2011). GSK189254 (6-[(3-cyclobutyl-2,3,4,5-tetrahydro-1H-3-benzazepin-7-yl)oxy]-N-methylpyridine-3-carboxamide) was purchased from Advanced ChemBlocks Inc. (Burlingame, CA). All other ligands were synthesized in house as previously described (van der Goot et al., 1992; Jansen et al., 1994; Vollinga et al., 1994, 1995; De Esch et al., 1999; Jablonowski et al., 2003; Lim et al., 2006, 2009; Smits et al., 2008). NanoGlo was obtained from Promega (Madison, WI). Fetal bovine serum was obtained from Bodinco (Alkmaar, The Netherlands), and penicillin/streptomycin was purchased from GE Healthcare (Uppsala, Sweden). Hanks' balanced salt solution (HBSS) was obtained from Gibco (Thermo Fisher Scientific, Waltham, MA). The cAMP-responsive element (CRE)–driven luciferase reporter gene plasmid pTLNC-21CRE was kindly provided by Dr. Born (National Jewish Medical and Research Center, Denver, CO), whereas the BRET-based cAMP biosensor plasmid pcDNA3.1-(L)-His-CAMYEL (cAMP sensor using YFP-Epac-RLuc, #ATCC-MBA-277) was purchased from the American Type Culture Collection (Manassas, VA). All other chemicals were bought from standard commercial resources and were of analytical grade.

Cloning of Nluc-hH_3R and Nluc-hH_4R Fusion Constructs. The start codons of the human H_3R and H_4R [Genbank: AF140538 (Lovenberg et al., 1999) and AY136745, respectively] were substituted with a *Kpn*2I restriction site sequence using polymerase chain reaction. The cDNA plasmid encoding the membrane signal peptide of the $5HT_{3A}$ receptor fused to Nluc was a gift from Dr. Hill (University of Nottingham, Nottingham, UK) (Stoddart et al., 2018b). Flanking *Kpn*I and *Kpn*2I restriction sites were introduced at the 5′ and 3′ end of this signal peptide–Nluc cDNA by polymerase chain reaction, allowing in-frame fusion to the N terminus of hH_3R (Lovenberg et al., 1999) and hH_4R in the pcDEF3 mammalian expression vector (Goldman et al., 1996). All generated constructs were validated by sequencing (Eurofins Genomics, Ebersberg, Germany).

Cell Culture and Transfection. Human embryonic kidney 293T cells (HEK293T cells) were cultured in Dulbecco's modified Eagle's medium supplemented with 10% fetal bovine serum, penicillin (100 μg/ml), and streptomycin (50 μg/ml) at 37°C with 5% CO_2. HEK293T cells were seeded (2×10^6 cells/10 cm^2 dish) and transiently transfected the next day with indicated amounts of cDNA using 25 kDa linear polyethyleneimine (PEI). The total amount of cDNA was kept constant at 5 μg per dish by the addition of complementary amounts of pcDEF3 plasmid. DNA/PEI (1:4 ratio) mixtures were preincubated in 150 mM NaCl solution for 20 minutes at 22°C before addition to the cells (Nijmeijer et al., 2013a).

Radioligand-Binding Assays. HEK293T cells were transfected with 2.5 μg of DNA encoding for wild-type and Nluc-fused hH_3R or hH_4R. After 48 hours, cells were collected in phosphate-buffered saline (PBS) and centrifuged at 1900*g* for 10 minutes. The cell pellet was resuspended in 1 ml of PBS per culture dish and centrifuged at 1900*g* for 10 minutes. Supernatant was discarded and the cell pellet was stored at −20°C until the day of the experiment. Cells were resuspended in binding buffer (50 mM Tris-HCl, pH 7.4, 22°C) and disrupted using a Branson sonifier 250 (Boom bv., Meppel, The Netherlands) on the day of the experiment.

Saturation radioligand binding was performed on 100 μl of cell homogenates expressing the hH_3R, Nluc-hH_3R, hH_4R, or Nluc-hH_4R with increasing concentrations of [^{3}H]NAMH or [^{3}H]histamine for 2 hours at 25°C. Nonspecific binding was measured in the presence of 100 μM clobenpropit or 10 μM JNJ7777120 (1-[(5-chloro-1*H*-indol-2-yl)carbonyl]-4-methylpiperazine). Equilibrium competition binding was performed on 100 μl of cell homogenates expressing the hH_3R with ~2 nM [^{3}H]NAMH or expressing the hH_4R with ~10 nM [^{3}H]histamine in the absence and presence of increasing concentrations of unlabeled ligands for 2 hours at 25°C. Incubations were terminated by rapid filtration over a 0.5% PEI-coated 96-well GF/C filter plate followed by five rapid wash steps with ice-cold wash buffer (50 mM Tris-HCl, pH 7.4, 4°C) using a PerkinElmer 96-well Filtermate-harvester. The GF/C filter plates were dried at 55°C, and 25 μl of Microscint-O scintillation liquid (PerkinElmer, Groningen, The Netherlands) was added per well. Filter-bound radioactivity was measured using a Microbeta Wallac Trilux scintillation counter (PerkinElmer) after a 300-minute delay.

NanoBRET-Based Binding Assays. HEK293T cells were transfected with cDNA encoding 0.5 μg of Nluc-hH_3R or Nluc-hH_4R. The next day, cells were transferred to poly-L-lysine–coated black 96-well plates (50,000 cells/well) and grown for an additional 24 hours. Equilibrium saturation binding of fluorescent clo-BDY or FL-histamine to intact cells expressing Nluc-hH_3R and Nluc-hH_4R was measured in a total volume of 100 μl of HBSS for 2 hours at 25°C. Nonspecific binding was determined by 100 μM clobenpropit or 10 μM JNJ7777120 for Nluc-hH_3R and Nluc-hH_4R, respectively. To determine the affinity (pK_i) of unlabeled ligands for the Nluc-hH_3R or Nluc-hH_4R, the cells were incubated with 50 nM clo-BDY or 1 μM FL-histamine in combination with increasing concentrations of unlabeled ligands (ranging from 10^{-5} to 10^{-11} M) in HBSS for 2 hours at 25°C. Binding of clo-BDY and FL-histamine to the Nluc-hH_3R or Nluc-hH_4R was detected as a BRET ratio upon the addition of 3.2 μl/ml NanoGlo (Promega, Madison, WI) using the PHERAstar plate reader (BMG Labtech, Ortenberg, Germany) at 475 nm (15-nm bandpass) and >610 nm (longpass) for clo-BDY and 460 nm (80-nm bandpass) and 535 nm (15-nm bandpass) for FL-histamine.

To measure clo-BDY-binding kinetics, Nluc-hH_3R–expressing cells were preincubated with 3.2 μl/ml NanoGlo (Promega) in HBSS for 15 minutes. Next, for association assays, 50, 100, or 200 nM clo-BDY was added to the cells and nonspecific binding was measured in the presence of 100 μM clobenpropit. For the competition association assay, 100 nM clo-BDY was added in the absence and presence of unlabeled ligands (10- or 40-fold K_i) in a total volume of 200 μl. In the case of dissociation assays, cells were preincubated with 100 nM clo-BDY for 2 hours before initiation of the dissociation by addition of

10 μM clobenpropit. Clo-BDY binding to the Nluc-hH_3R was directly measured every minute for 2 hours using a PHERAstar plate reader (BMG) at 460 nm (80-nm bandpass) and >610 nm (longpass).

CRE-Luciferase Reporter Gene Assay. HEK293T cells were transiently transfected with 2.5 μg of CRE-luc DNA in combination with 50 ng of Nluc-hH_3R or 1000 ng of Nluc-hH_4R, hH_3R, or hH_4R DNA. The next day, cells were transferred to white poly-L-lysine–coated 96-well plates (50,000 cells/well) and grown for an additional 24 hours. The cells were stimulated with increasing ligand concentrations in the absence or presence of a single concentration of antagonist in Dulbecco's modified Eagle's medium supplemented with 1 μM forskolin at 37°C and 5% CO_2. The incubations were terminated after 6 hours by replacing the medium with 25 μl/well luciferase assay reagent [0.83 mM ATP, 0.83 mM d-luciferin, 18.7 mM $MgCl_2$, 0.78 μM Na_2PO_4, 38.9 mM Tris-HCl (pH 7.8), 0.39% glycerol, 0.03% Triton-X-100, and 2.6 μM dithiothreitol]. Luminescence was measured with a Mithras plate reader (Berthold, Bad Wildbad, Germany) after 30 minutes at 37°C.

hH_3R Functional Recovery Assay after Antagonist Washout. HEK293T cells were transfected with 0.5 μg of hH_3R and 3 μg of CAMYEL DNA (Scholten et al., 2012). The next day, cells were transferred to a poly-L-lysine–coated white 96-well plate and preincubated overnight with 1 μM hH_3R antagonist pitolisant or ABT-239 at 37°C. Next, cells were washed twice with PBS at different time points and allowed to re-equilibrate in HBSS at 37°C. The cells were incubated with 5 μM coelenterazine-h and 40 μM 3-isobutyl-1-methylxanthine for 5 minutes, followed by a stimulation with 1 μM histamine. After 10 minutes, 1 μM forskolin was added and luminescence was measured at 480 nm (20-nm bandpass) (RLuc) and 540 nm (40-nm bandpass) (BRET) using the Mithras multimode reader.

Data Analysis. Data were analyzed using GraphPad Prism 7.02 (GraphPad Software, San Diego, CA). Data shown are means ± S.D. of at least three independent experiments performed in triplicate, unless stated differently. BRET ratio was calculated by dividing the fluorescent acceptor signal by the signal of the luminescent donor. Competition-binding curves were fitted to a one-sited binding model to quantify the IC_{50} value, and equilibrium dissociation constants (K_i) of unlabeled ligands were subsequently calculated using the Cheng-Prusoff equation (see equation 1) (Cheng and Prusoff, 1973):

$$K_i = \frac{IC_{50}}{1 + {[L]}/{K_D}} \tag{1}$$

where $[L]$ is the concentration of labeled ligand, and K_D is the equilibrium dissociation constant of the labeled ligand.

Association and dissociation data were fitted and subjected to an extra-sum-of square F-test to compare between one- or two-phase association and one- or two-phase exponential decay models. Competition association curves were fitted to Motulsky and Mahan model (see equation 2) (Motulsky and Mahan, 1984):

$$\begin{aligned} K_a &= k_1[L] + k_2 \\ K_b &= k_3[I] + k_4 \\ S &= \sqrt{(K_a - K_b)^2 + 4 \cdot k_1 \cdot k_3 \cdot [L] \cdot [I]} \\ K_F &= 0.5(K_a + K_b + S) \\ K_s &= 0.5(K_a + K_b - S) \\ Q &= \frac{B_{max} \cdot k_1 \cdot L}{K_F - K_S} \\ Y &= Q \cdot \frac{(k_4 \cdot (K_F - K_S)}{K_F \cdot K_S} + \frac{k_4 - K_F}{K_F} e^{(-k_F \cdot X)} - \frac{k_4 - K_S}{K_S} e^{(-K_S \cdot X)} \end{aligned} \tag{2}$$

where k_1 and k_3 ($M^{-1} \cdot min^{-1}$) are the association rate constants (k_{on}), whereas k_2 and k_4 (min^{-1}) are the dissociation rate constants (k_{off}) of labeled and unlabeled ligand, respectively; $[L]$ and $[I]$ are the concentrations of labeled and unlabeled ligand, respectively; B_{max} is the maximum specific binding sites; and Y is the specific binding.

Kinetic "K_D" was calculated according to eq. 3:

$$\text{kinetic } K_D = \frac{k_{off}}{k_{on}} \tag{3}$$

Residence time (RT) indicates how long a ligand stays bound to its receptor (Copeland et al., 2006; Hoffmann et al., 2015; Copeland, 2016) and was calculated using eq. 4:

$$RT = \frac{1}{k_{off}} \tag{4}$$

The correlation between data sets was analyzed by Deming regression, and the Pearson correlation coefficient (r^2) was calculated using GraphPad Prism 7.02.

Results

Pharmacological Characterization of Nluc-Tagged hH_3R and hH_4R. To confirm that the N-terminally fused Nluc does not affect hH_3R and hH_4R function, radioligand saturation binding was measured on HEK293T cell homogenates transiently expressing Nluc-hH_3R or Nluc-hH_4R and compared with binding to their wild-type counterparts. The radioligand [^{3}H]NAMH displayed similar ($P = 0.38$, Student's t test) affinities for the wild-type hH_3R ($K_D = 1.37 \pm 0.3$ nM, $B_{max} = 1.5 \pm 0.4$ pmol/mg, $n = 5$) and the Nluc-hH_3R ($K_D = 1.78 \pm 0.8$ nM, $B_{max} = 11 \pm 10$ pmol/mg, $n = 7$), indicating that N-terminal fusion to Nluc does not significantly affect the orthosteric hH_3R ligand-binding site (Fig. 1A). Likewise, saturation binding of [^{3}H]histamine to wild-type hH_4R and Nluc-hH_4R revealed similar ($P = 0.22$, Student's t test) K_D values of 4.4 ± 0.6 nM ($n = 3$) and 2.9 ± 1.4 nM ($n = 3$), respectively, even though Nluc-hH_4R expression was lower ($B_{max} = 5.6 \pm 1.4$ pmol/mg and 1.3 ± 0.4 pmol/mg for hH_4R and Nluc-hH_4R, respectively) (Fig. 1B).

Stimulation of HEK293T cells transiently expressing Nluc-hH_3R or Nluc-hH_4R with histamine resulted in a concentration-dependent inhibition of 1 μM forskolin-induced CRE reporter gene activity with potency (pEC_{50}) values of 8.6 ± 0.1 and 8.3 ± 0.3, respectively, confirming that N-terminal Nluc fusion to these receptors did not affect their signaling capacity as compared with wild-type hH_3R ($pEC_{50} = 8.7 \pm 0.1$) and hH_4R ($pEC_{50} = 8.2 \pm 0.2$) (data not shown). In contrast, the fluorescent ligand FL-histamine (Supplemental Fig. 1) did not induce Nluc-hH_3R or Nluc-hH_4R–mediated inhibition of forskolin-induced CRE reporter gene activity. Clobenpropit acted as an antagonist and full agonist at the Nluc-hH_3R ($\alpha = 0.0$) and Nluc-hH_4R ($pEC_{50} = 8.8 \pm 0.4$, $\alpha = 1.0 \pm 0.1$), respectively (Fig. 1, C and D), although previously reported for wild-type hH_3R as an inverse agonist and hH_4R agonist (Lim et al., 2005). Its fluorescent derivative clo-BDY (structure not disclosed by manufacturer) acted as an antagonist at Nluc-hH_3R and full agonist ($pEC_{50} = 8.0 \pm 0.1$, $\alpha = 1.0 \pm 0.0$) at Nluc-hH_4R (Fig. 1, C and D). Indeed, hH_3R-mediated inhibition of forskolin-induced CRE reporter gene activity in response to increasing concentrations of histamine was antagonized by 5 μM FL-histamine or 1 μM clo-BDY, resulting in a parallel right shift of the histamine concentration-response curve (Supplemental Fig. 2A). Surprisingly, FL-histamine (10 μM) did not affect hH_4R-mediated CRE reporter gene activity in response to increasing concentrations of histamine (Supplemental Fig. 2B), suggesting that FL-histamine does not interact with the hH_4R.

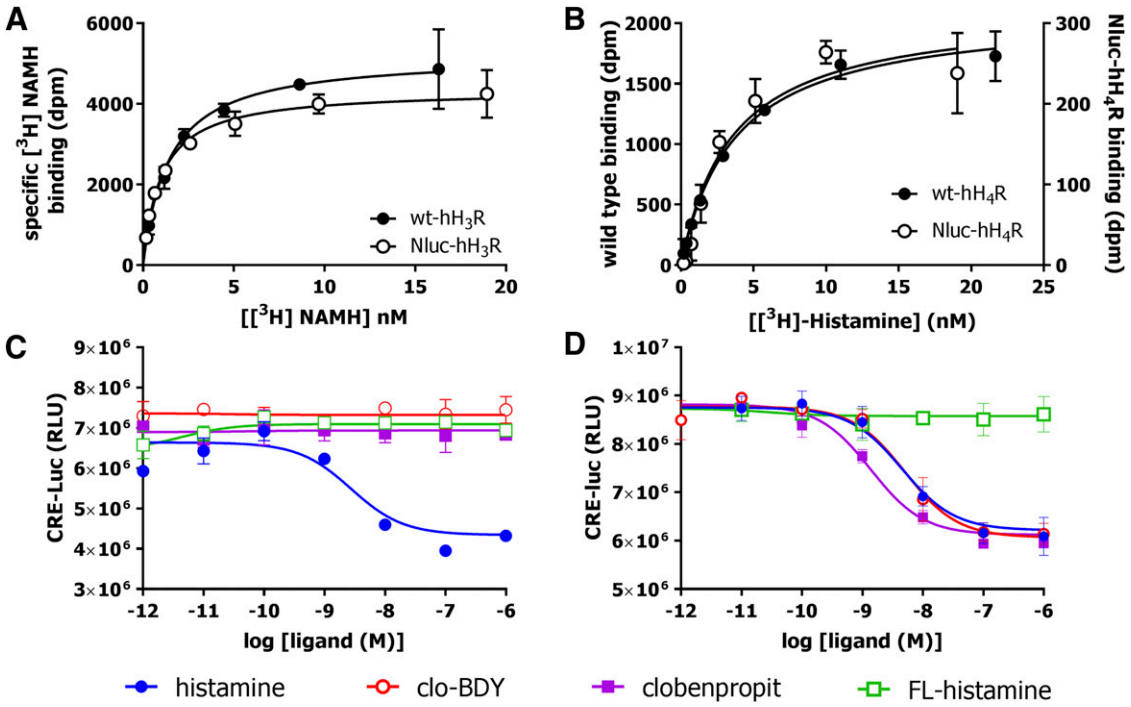

Fig. 1. Pharmacological characterization of Nluc-fused hH_3R and hH_4R. (A) Specific binding of [^{3}H]NAMH to HEK293T cell homogenates expressing wild-type (wt) hH_3R or Nluc-hH_3R. (B) Specific binding of [^{3}H]histamine to HEK293T cell homogenates expressing wild-type hH_4R or Nluc-hH_4R. Ligand-induced Nluc-hH_3R (C) and Nluc-hH_4R (D) activation as measured by CRE-luc reporter gene assay in transiently cotransfected HEK293T cells. Representative graphs of at least three experiments performed in triplicate are shown. RLU, relative luminescence units.

NanoBRET-Based Saturation and Competition Binding on Intact Cells Expressing Nluc-hH_3R and Nluc-hH_4R. Binding of red fluorescent clo-BDY or green fluorescent FL-histamine to living intact HEK293T cells expressing either Nluc-hH_3R or Nluc-hH_4R was quantified as NanoBRET between the luminescent Nluc donor and the fluorescent BODIPY acceptor moiety. Incubation of cells expressing either Nluc-hH_3R or Nluc-hH_4R for 2 hours at 25°C with increasing concentrations of clo-BDY resulted in a saturable increase in NanoBRET signals under equilibrium conditions, resulting in K_D values of 13 ± 1.9 and 70 ± 30 nM for Nluc-hH_3R and Nluc-hH_4R, respectively (Fig. 2, A and C). Saturation binding of FL-histamine displayed moderate affinity K_D = 427 ± 87 nM for the Nluc-hH_3R (Fig. 2E). Surprisingly, no specific binding could be observed on cells expressing the Nluc-hH_4R if tested up to a concentration of 10 μM (data not shown), which is in contrast to the previously reported FL-histamine binding to hH_4R on murine bone marrow–derived mast cells with a K_D of 2.1 μM as measured by flow cytometry (Mirzahosseini et al., 2015).

Coincubation of a single concentration of clo-BDY (50 nM) or FL-histamine (1 μM) in combination with a selection of unlabeled ligands and cells expressing either Nluc-hH_3R or Nluc-hH_4R for 2 hours at 25°C resulted in a concentration-dependent decrease in NanoBRET by histamine and clobenpropit, indicating that these unlabeled ligands compete with the fluorescent ligand for binding to both the Nluc-hH_3R and Nluc-hH_4R (Fig. 2, B, D, and F). In contrast, the hH_3R-selective antagonist pitolisant only competed with clo-BDY and FL-histamine for binding to Nluc-hH_3R (Fig. 2, B and F) but not for the binding of clo-BDY to Nluc-hH_4R (Fig. 2D). This selectivity profile toward H_3R was previously observed in radioligand-binding studies on wild-type hH_3R and hH_4R (Ligneau et al., 2007). Oppositely, the hH_4R-selective antagonist JNJ7777120 only displaced clo-BDY from Nluc-hH_4R (Fig. 2D) but hardly from Nluc-hH_3R (Fig. 2B), which is in line with its previously reported 300-fold lower affinity for the H_3R compared with the H_4R (Lim et al., 2005).

Binding affinities (pK_i) of unlabeled ligands for Nluc-hH_3R and Nluc-hH_4R were calculated from the NanoBRET-based competition-binding assays using the Cheng-Prusoff equation (Cheng and Prusoff, 1973) and subsequently compared with pK_i values that were derived from radioligand competition binding to wild-type hH_3R or hH_4R (Table 1). A clear difference is observed between agonists and antagonists in the linear correlation of their pK_i values for the hH_3R obtained in competition with either clo-BDY or [^{3}H]NAMH (Fig. 3A). Agonists consistently displayed lower binding affinities in the NanoBRET-based binding assay as compared with the radioligand-binding assay with a correlation of r^2 = 0.8556 (P = 0.003). In contrast, antagonists tended to display more comparable affinities for hH_3R and Nluc-hH_3R in both assay formats with a correlation of r^2 = 0.8008 (P = 0.015). A similar difference in agonist affinities for the hH_3R is observed when comparing FL-histamine with [^{3}H]NAMH competition-binding curves. Again, antagonists tended to display more comparable pK_i values in both NanoBRET- and radioligand-based assays (Supplemental Table 1). Indeed, pK_i values of unlabeled ligands obtained with either "red" tracer clo-BDY or "green" tracer FL-histamine in Nluc-hH_3R competition-binding assays showed a high overall linear correlation (r^2 = 0.9794, $P < 0.0001$) (Fig. 3B).

The NanoBRET-based hH_4R competition-binding assays on intact cells yielded lower pK_i values for all tested ligands as compared with radioligand competition-binding assays on cell homogenates (Table 1). Yet, a correlation was observed for the pK_i values of both agonists (r^2 0.7673, P = 0.004) and antagonists (r^2 0.9184, P = 0.01) between the two hH_4R-binding assay formats (Fig. 3C).

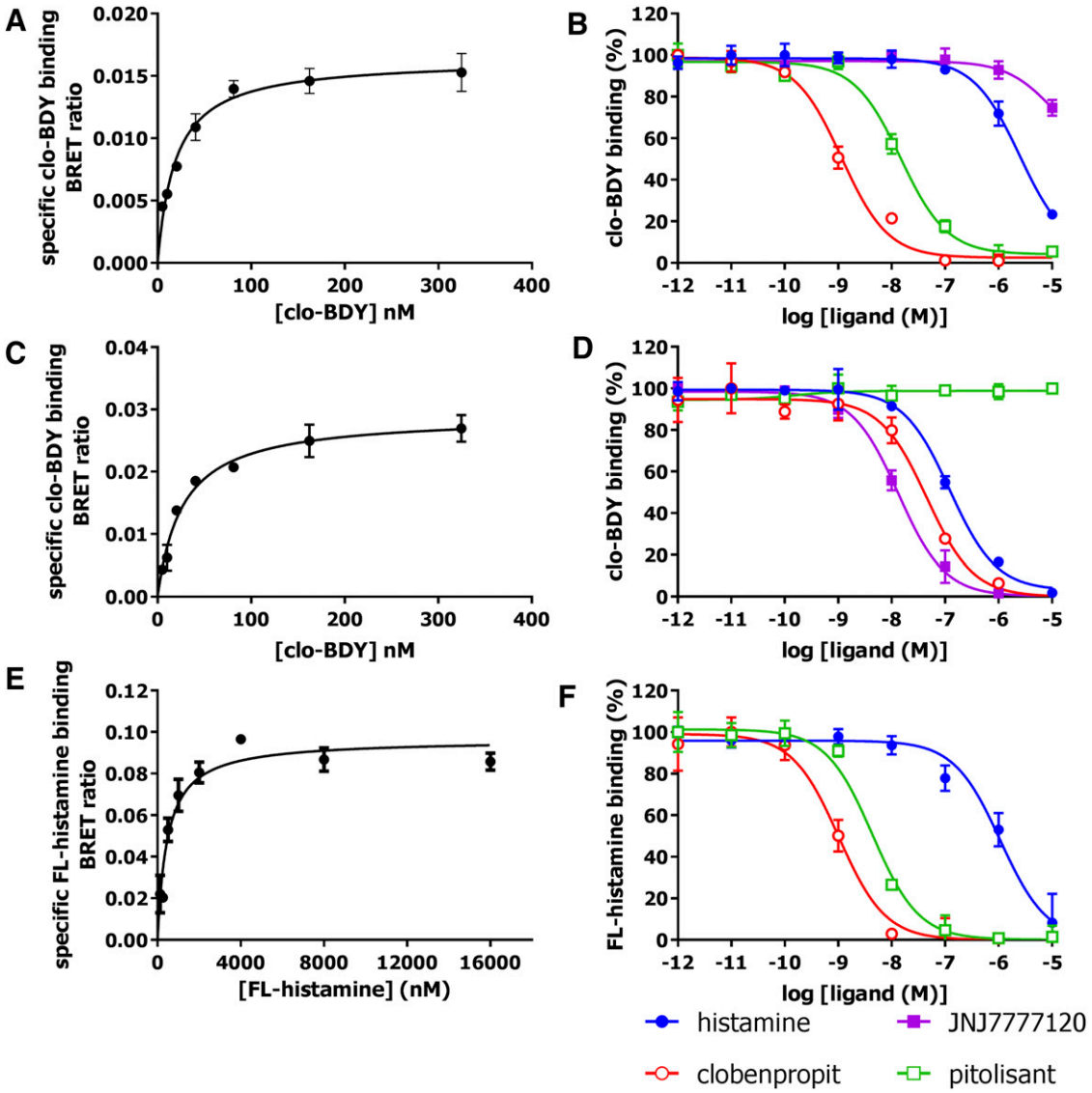

Fig. 2. NanoBRET equilibrium saturation binding of clo-BDY on Nluc-hH_3R (A), Nluc-hH_4R (C), and FL-histamine on Nluc-hH_3R (E) transiently expressed on intact HEK293T cells. NanoBRET competition binding of clo-BDY to the Nluc-hH_3R (B) and Nluc-hH_4R (D), and FL-histamine on Nluc-hH_3R (F) transiently expressed on intact HEK293T cells. Representative graphs of at least three experiments performed in triplicate are shown.

Binding Kinetics of Fluorescent Clo-BDY on Nluc-hH_3R Measured by NanoBRET. As both clo-BDY and FL-histamine display similar binding affinities of unlabeled ligands in equilibrium competition binding, clo-BDY was selected as a fluorescent ligand for real-time detection of ligand binding due to its higher affinity and smaller spectral overlap with NanoLuc. Real-time detection of NanoBRET upon the addition of three concentrations (approximately 4×, 8×, and 16× K_D) of clo-BDY to intact HEK293T cells expressing Nluc-hH_3R at 25°C revealed monophasic association binding of clo-BDY to the Nluc-hH_3R with globally fitted k_{on} and k_{off} values of 2.0 ± 1.4 × 10^5 M^{-1}·min^{-1} and 0.048 ± 0.02 min^{-1}, respectively (Fig. 4A). The reciprocal of the k_{off} value indicated that clo-BDY has an RT of 23 ± 8.0 minutes on the Nluc-hH_3R. Calculation of the equilibrium dissociation constant from the ratio of k_{off} to k_{on} ($K_D = k_{off}/k_{on}$) revealed a 39-fold lower "kinetic" K_D value (= 513 ± 272 nM) of clo-BDY for Nluc-hH_3R as compared with its K_D (= 13 ± 1.9 nM) obtained from the saturation binding curve at equilibrium (Fig. 2A).

Binding Kinetics of Unlabeled Ligands on Nluc-hH_3R Measured by NanoBRET. Real-time measurement of the binding of clo-BDY (100 nM) to the Nluc-hH_3R in the absence and presence of unlabeled hH_3R ligands allowed the determination of the binding rate constants of the latter by using the Motulsky and Mahan method (Motulsky and Mahan, 1984). A shallow initial overshoot followed by a lower clo-BDY "steady-state" binding to Nluc-hH_3R was observed in the presence of 10 nM (40× K_i) unlabeled clobenpropit, which indicates slower dissociation kinetics for unlabeled clobenpropit to the Nluc-hH_3R as compared with clo-BDY (Fig. 4B). In contrast, clo-BDY binding to Nluc-hH_3R gradually reached equilibrium in the presence of 5011 nM (10× K_i) unlabeled histamine, indicating that this endogenous hH_3R agonist has faster receptor-binding kinetics for the Nluc-hH_3R in comparison with clo-BDY (Fig. 4C). Indeed, unlabeled clobenpropit and histamine had 1.8-fold lower and 1.9-fold higher k_{off} values, respectively, as compared with clo-BDY (Table 2), resulting in a proportionally longer (44 ± 21 minutes) and shorter

TABLE 1

Affinity of H_3 and H_4 ligands on the wild-type hH_3R (wt-hH_3R) and wt-hH_4R using radioligand and Nluc-hH_3R and Nluc-hH_4R using NanoBRET-based competition binding assays

Data represent the mean ± S.D. of at least three experiments performed in triplicate.

Compound	Nluc-hH_3R	wt-hH_3R	Action[a]	Compound	Nluc-hH_4R	wt-hH_4R	Action[a]
	pK_i vs. clo-BDY	pK_i vs. [^{3}H]NAMH			pK_i vs. clo-BDY	pK_i vs. [^{3}H]histamine	
Histamine	6.3 ± 0.2*	7.9 ± 0.3	A	Histamine	6.8 ± 0.3*	7.9 ± 0.2	A
NAMH	7.8 ± 0.2*	8.8 ± 0.1	A	VUF8430	6.8 ± 0.3*	7.5 ± 0.1[b]	A
Imetit	8.3 ± 0.4*	9.7 ± 0.4	A	Imetit	7.4 ± 0.1*	8.4 ± 0.3	A
SAMH	6.4 ± 0.4*	7.6 ± 0.8	A	VUF8328	7.6 ± 0.2*	8.4 ± 0.1	A
Immepip	8.5 ± 0.5*	9.3 ± 0.1	A	VUF4656	7.5 ± 0.1*	8.8 ± 0.1[b]	A
Dimaprit	5.9 ± 0.3	6.1 ± 0.2	A	VUF5228	5.9 ± 0.3*	7.3 ± 0.2[b]	A
VUF5524	6.6 ± 0.2*	7.5 ± 0.1	A	4-methylhistamine	6.4 ± 0.2*	7.3 ± 0.1[b]	A
Clobenpropit	9.6 ± 0.1	10.0 ± 0.4	I	Clobenpropit	7.4 ± 0.3*	8.0 ± 0.1	A
Thioperamide	7.3 ± 0.3	7.2 ± 0.2	I	Thioperamide	7.2 ± 0.4	7.5 ± 0.2	I
Iodophenpropit	8.9 ± 0.4	9.2 ± 0.4	I	Iodophenpropit	7.6 ± 0.2*	8.2 ± 0.3	I
A-331440	7.7 ± 0.4*	8.6 ± 0.1	I	VUF6002	7.1 ± 0.3	7.7 ± 0.1[b]	I
A-349821	9.7 ± 0.6	9.7 ± 0.0	I	VUF10499	6.8 ± 0.2*	7.3 ± 0.1	I
Pitolisant	8.6 ± 0.0*	8.0 ± 0.2	I	Pitolisant	<5	ND	ND
JNJ7777120	<5	5.3 ± 0.1[b]	ND	JNJ7777120	7.9 ± 0.2	8.2 ± 0.1	I

A, agonist; I, antagonist/inverse agonist in CRE-luciferase reporter gene or guanosine 5′-*O*-(3-[^{35}S]thio)triphosphate ([^{35}S]GTPγS) assay, ND, not determined; VUF10499, 6-chloro-N-(furan-3-ylmethyl)2-(4-methylpiperazin-1-yl)quinazolin-4-amine; VUF4656, 3-(1H-imidazol-4-yl)propyl (3,4-dichlorobenzyl)carbamimidothioate dihydrobromide; VUF5228, 3-(1H-imidazol-4-yl)propyl (E)-N-(4-chlorobenzyl)-N′-cyclohexylcarbamimidothioate dihydrobromide; VUF5524, 4-pentyl-1H-imidazole oxalate; VUF6002, 5-chloro-2-((1-methylpiperidin-4-ylidene)methyl)-1H-benzo[d]imidazole; VUF8328, 3-(1H-imidazol-4-yl)propyl carbamimidothioate dihydrobromide; VUF8430, 2-guanidinoethyl carbamimidothioate dihydrobromide.

[a]Action obtained from Lim et al. (2005), Bongers et al. (2007), and Nijmeijer et al. (2013b).

[b]pK_i values obtained from Lim et al. (2005) and Nijmeijer et al. (2013); data are the mean ± S.E.M.

*Significant differences in pK_i values between the NanoBRET-based and radioligand binding assays ($P < 0.05$) as determined by Student's *t* test.

(12 ± 3.8 minutes) RT on Nluc-hH_3R than clo-BDY. The agonists imetit and NAMH displayed faster binding kinetics as compared with clo-BDY, with RT values of 18 ± 12 and 18 ± 7.4 minutes, respectively (Table 2). The antagonist thioperamide displayed comparably slow binding kinetics as unlabeled clobenpropit, whereas antagonists A-331440 and [4′-{3-([R,R]2,5-dimethyl-pyrrolidin-1-yl)-propoxy}-biphenyl-4-yl]-morpholin-4-yl-methanone (A-349821) bound the Nluc-hH_3R with faster kinetics and RTs of 20 ± 14.6 and 17 ± 6.7 minutes, respectively (Table 2). In this assay, the k_{off} value (0.066 ± 0.02 minute^{-1}) of unlabeled A-349821 on intact HEK293T cells was similar to the previously observed dissociation rate constant for the dissociation of pre-bound [^{3}H]A-349821 from membranes of hH_3R-expressing C6 cells (Witte et al., 2006).

The only currently marketed hH_3R-targeting antagonist, pitolisant (Wakix), bound the Nluc-hH_3R with relatively fast kinetics (k_{on} = 1.4 ± 1.0 × 10^6 M^{-1}·min^{-1} and k_{off} = 0.086 ± 0.07 minute^{-1}), resulting in an RT of 17 ± 10 minutes (Fig. 4D; Table 3). Interestingly, considerable variation was observed in the target residence time of five hH_3R antagonists that have been or are currently in clinical trials. The RT of bavisant (Fig. 4E) and PF-03654746 was in the same range as pitolisant, with RT values of 8.4 ± 2.3 and 15 ± 4.1 minutes, respectively (Table 3). In contrast, considerably longer residence times for binding to Nluc-hH_3R were observed for GSK1004723 (59 ± 83 minutes) and ABT-239 (75 ± 52 minutes), resulting in an initial overshoot of clo-BDY binding to Nluc-hH_3R (Fig. 4F).

The "kinetic pK_D" calculated from the observed k_{on} and k_{off} values of the unlabeled ligands in the competitive association-binding assay revealed a linear relationship (r^2 = 0.7398, P = 0.0007) with the corresponding pK_i values that were derived from competition-binding curves under equilibrium conditions using the same NanoBRET technology (Fig. 5A; Tables 2 and 3). However, the calculated kinetic pK_D values were up to 50-fold lower than the observed pK_i (Fig. 5A). Interestingly, ligand affinity (pK_i) of unlabeled ligands was linearly correlated (r^2 = 0.7789, P = 0.0003) to the log k_{on} (Fig. 5B), but no correlation (r^2 = 0.067, P = 0.441) was found between pK_i and log k_{off} values (Fig. 5C), suggesting that the on-rate of ligands drives hH_3R affinity (Sykes et al., 2009; Guo et al., 2016).

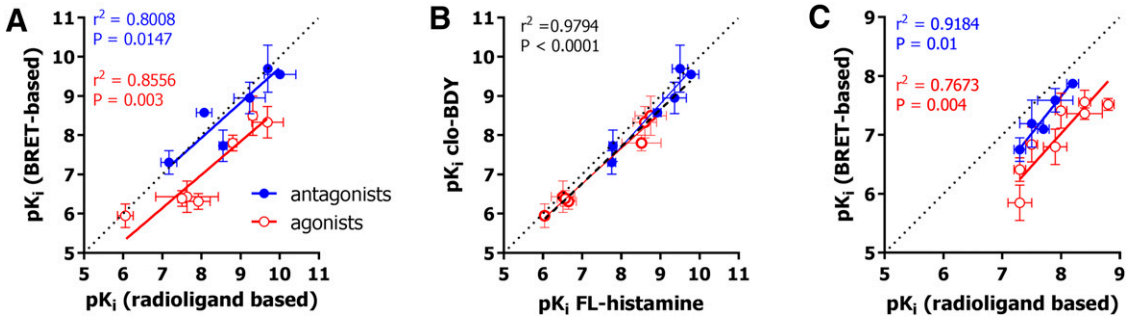

Fig. 3. Correlation plots of equilibrium dissociation constants (pK_i) of ligands for Nluc-hH_3R (A and B) and Nluc-hH_4R (C) as obtained by radioligand or NanoBRET-based competition-binding assays. Correlation of radioligand- and NanoBRET-based pK_i values as determined by clo-BDY as tracer (A and C). (B) Correlation between pK_i of ligands measured in a NanoBRET-based competition binding assay versus fluorescent clo-BDY or FL-histamine on Nluc-hH_3R. Deming linear regression was used for data fitting, and dotted line shows line of unity.

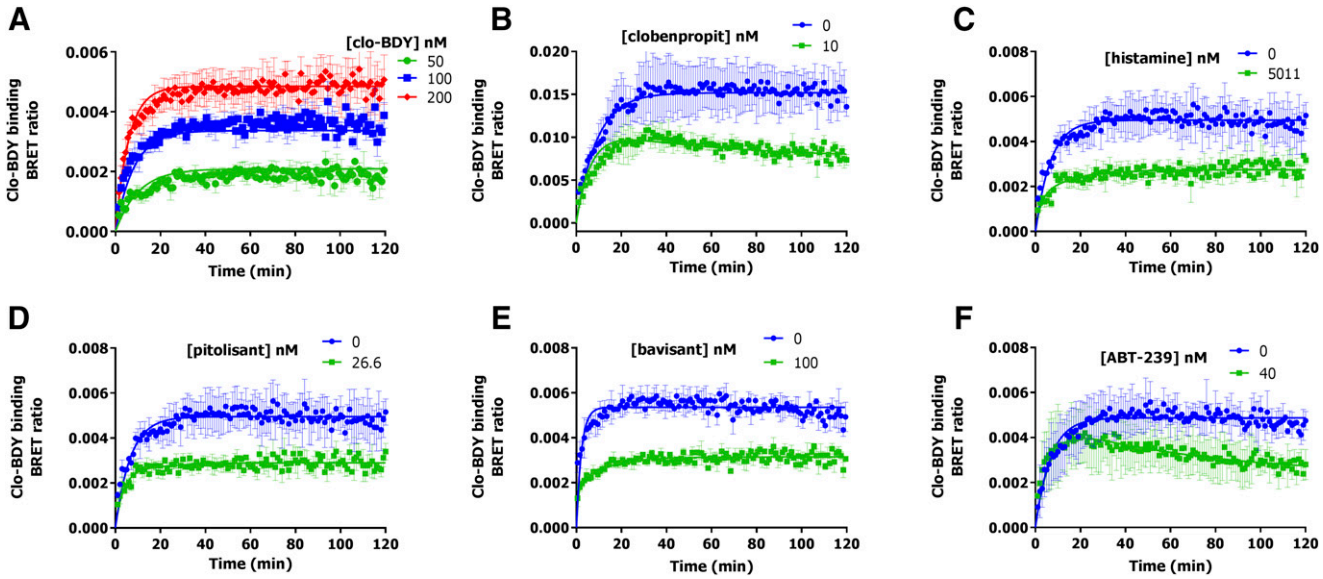

Fig. 4. Real-time detection of clo-BDY binding to Nluc-hH_3R by NanoBRET. (A) Association of three concentrations of clo-BDY. Competition association assay of 100 nM clo-BDY in competition with clobenpropit (B), histamine (C), pitolisant (D), bavisant (E), and ABT-239 (F) on the Nluc-hH_3R transiently expressed on HEK293T cells at 25°C. Representative graphs of at least three experiments performed in triplicate are shown.

Plotting the logarithm of k_{on} versus the k_{off} values illustrates that ligands with the same affinity, as indicated by the diagonal lines, can have considerably different kinetics (Fig. 5D).

Duration of Functional hH_3R Antagonism. Next, the duration of H_3R antagonism was functionally measured upon induction of prebound antagonist dissociation by washout of unbound ligand to evaluate the impact of the RT ($= 1/k_{off}$) derived from the NanoBRET competitive association assay. To this end, the recovery rate of hH_3R responsiveness to histamine (1 μM) stimulation was measured in transiently transfected HEK293T cells by using the cAMP-sensitive BRET-based biosensor CAMYEL at 37°C. Overnight preincubation with 1 μM hH_3R antagonists pitolisant or ABT-239 (pK_i values were 8.6 ± 0.0 and 9.0 ± 0.2, respectively, in NanoBRET-based binding on intact cells) followed by a washout of unbound antagonist resulted in a full recovery of hH_3R responsiveness for the short-RT (17 minutes) antagonist pitolisant within 1.5 hours. In contrast, the prebound long-RT (75 minutes) antagonist ABT-239 showed a much-slower recovery of hH_3R responsiveness to histamine stimulation, and 60% of hH_3R-mediated signaling was still blocked 4.5 hours after its dissociation was initiated (Fig. 6).

Discussion

The availability of fluorescent ligands in combination with the recently engineered Nluc luciferase allows the development of NanoBRET-based ligand-receptor-binding assays (Stoddart et al., 2015, 2018a,b; Soave et al., 2016). Since NanoBRET only occurs if the fluorescent ligand is bound to the Nluc-tagged GPCR, this assay can be performed in a homogeneous format without additional washing steps to separate unbound from bound fluorescent ligand and is, therefore, well suited to detect real-time ligand binding to GPCRs that are expressed on living cells. Quantification of binding parameters of a ligand for its GPCR on living cells is functionally more relevant as compared with measurements on membrane preparations or cell homogenates, as used buffer and intracellular interacting proteins can affect the latter assays (Emami-Nemini et al., 2013; Vauquelin et al., 2015; Bosma et al., 2017; Vanderheyden and Benachour, 2017; Stoddart et al., 2018). Here, a NanoBRET-based binding assay for the Nluc-hH_3R and Nluc-hH_4R on intact cells was developed utilizing the commercially available fluorescent ligands clo-BDY and FL-histamine.

As shown in this study, unlabeled agonists displayed higher affinity for the hH_3R in cell homogenates as determined by

TABLE 2

Kinetic parameters of unlabeled ligands, determined by competition association assays of clo-BDY to Nluc-hH_3R

Data represent the mean ± S.D. of at least three experiments performed in triplicate.

Compound	k_{on} (M^{-1}·min^{-1})	k_{off} (min^{-1})	RT (min)	Kinetic "pK_D"	pK_i[a]
Histamine	8.0 ± 7.3 × 10^4	0.089 ± 0.02	12 ± 3.8	5.8 ± 0.4	6.3 ± 0.2
NAMH	1.6 ± 0.3 × 10^5	0.062 ± 0.02	18 ± 7.4	6.6 ± 0.4	7.8 ± 0.2
Imetit	9.1 ± 8.7 × 10^5	0.092 ± 0.07	17 ± 12	6.9 ± 0.5	8.3 ± 0.4
Clobenpropit	1.4 ± 0.6 × 10^7	0.026 ± 0.01	44 ± 21	8.7 ± 0.1	9.6 ± 0.1
Thioperamide	1.6 ± 2.0 × 10^6	0.026 ± 0.01	41 ± 12	7.5 ± 0.4	7.3 ± 0.3
A-331440	2.3 ± 3.0 × 10^5	0.078 ± 0.05	20 ± 14	6.3 ± 0.3	7.7 ± 0.4
A-349821	1.6 ± 1.1 × 10^7	0.066 ± 0.02	17 ± 6.7	8.3 ± 0.4	9.7 ± 0.6

[a]pK_i values as determined in NanoBRET displacement assay (Table 1).

TABLE 3

Kinetic parameters of H_3R drug candidates, determined by competition association assay with clo-BDY on the Nluc-hH_3R

Data represent the mean ± S.D. of at least three experiments performed in triplicate.

Compound	k_{on} ± S.D. ($M^{-1}\cdot min^{-1}$)	k_{off} ± S.D. (min^{-1})	RT (min)	Kinetic "pK_D"	pK_i[a]
Pitolisant	$1.4 \pm 1.0 \times 10^6$	0.086 ± 0.07	17 ± 10	7.2 ± 0.3	8.6 ± 0.0
Bavisant	$7.0 \pm 4.8 \times 10^5$	0.13 ± 0.04	8.4 ± 2.3	6.7 ± 0.3	8.6 ± 0.4
GSK189254	$1.3 \pm 1.8 \times 10^7$	0.024 ± 0.01	44 ± 11	8.4 ± 0.7	9.6 ± 0.3
GSK1004723	$2.3 \pm 2.1 \times 10^5$	0.037 ± 0.03	59 ± 83	6.7 ± 0.2	8.0 ± 0.1
PF-03654746	$4.4 \pm 1.2 \times 10^6$	0.073 ± 0.02	15 ± 4.1	7.8 ± 0.1	9.3 ± 0.4
ABT-239	$9.2 \pm 5.4 \times 10^5$	0.017 ± 0.01	75 ± 52	7.7 ± 0.1	9.0 ± 0.5

[a]pKi obtained from NanoBRET assay (Table 1).

[^{3}H]NAMH displacement in comparison with the NanoBRET-based binding assay on intact cells. Indeed, higher-affinity agonist-bound GPCR ternary complexes can be formed in membrane preparations or cell homogenates with their associated G protein in the absence of free guanine nucleotides, as compared with the more-transient ternary complexes in intact cells resulting in lower agonist-binding affinities (Witte et al., 2006; Strange, 2008; Chabre et al., 2009; Emami-Nemini et al., 2013). Interestingly, a similar difference in the affinity of unlabeled agonists for the hH_3R was observed in competition-binding experiments on cell homogenates using agonist [^{3}H]NAMH versus antagonist [^{125}I]iodophenpropit as radioligands (Bongers et al., 2007). Comparison of pK_i values of unlabeled ligands derived from the NanoBRET-based competition binding using the fluorescent antagonist clo-BDY with those obtained from [^{125}I]iodophenpropit displacement revealed similar binding affinities in both assay formats (r^2 0.9239, $P < 0.0001$) without an obvious discrepancy between unlabeled H_3R agonists and H_3R antagonists (Fig. 7). In contrast to the [^{3}H]NAMH-binding assay, both NanoBRET-based clo-BDY and [^{125}I]-iodophenpropit competition binding assays are performed in buffers containing near-physiologic (~140 mM) NaCl

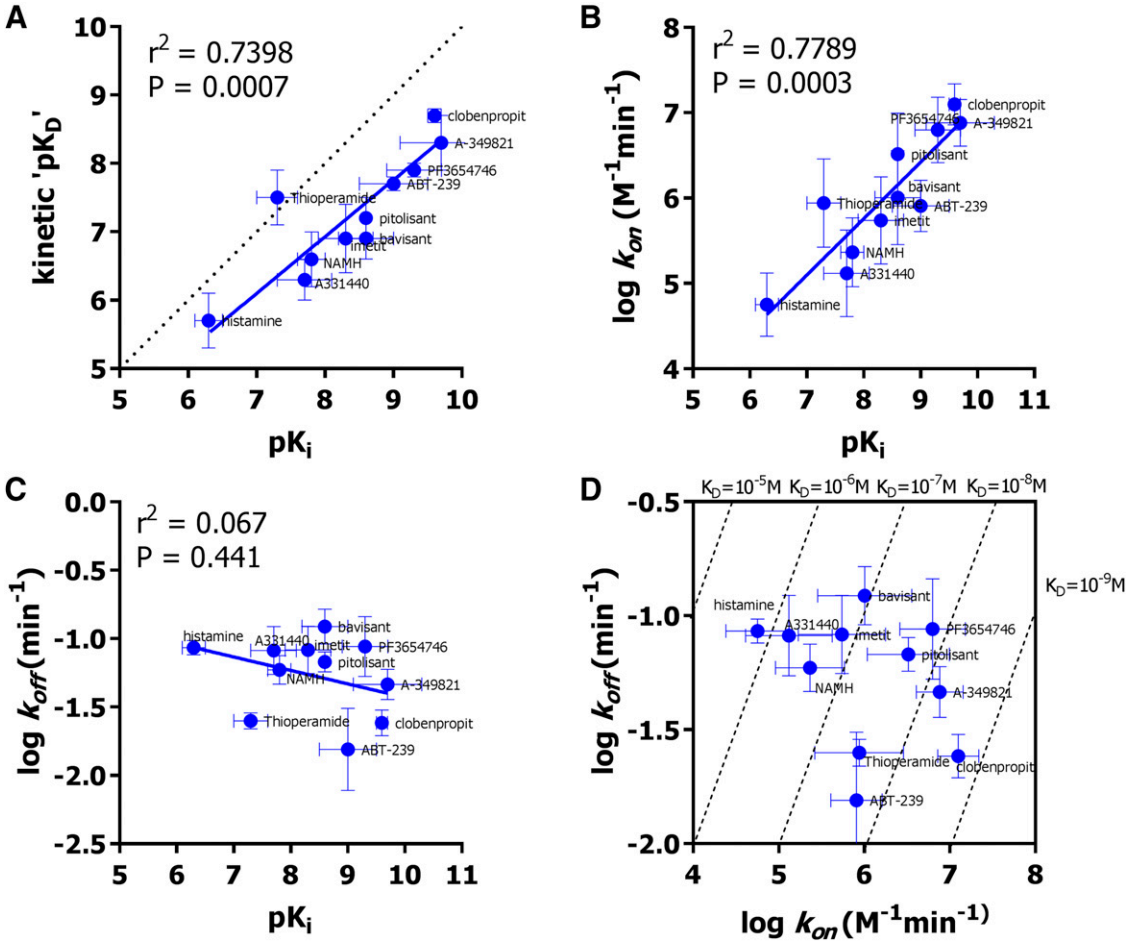

Fig. 5. Comparison of the affinity (pK_i) of unlabeled ligands for the Nluc-hH_3R obtained from equilibrium NanoBRET assays with their association and dissociation rate constants and kinetic "pK_D" from real-time measurements (Table 2). Deming linear regression was used for data fitting of pK_i versus pK_D (A), pK_i versus log k_{on} (B), and pK_i versus log k_{off} (C). Distribution of log k_{on} versus log k_{off} in relation to their kinetic "K_D" as represented by diagonal lines (D). Dotted line shows line of unity.

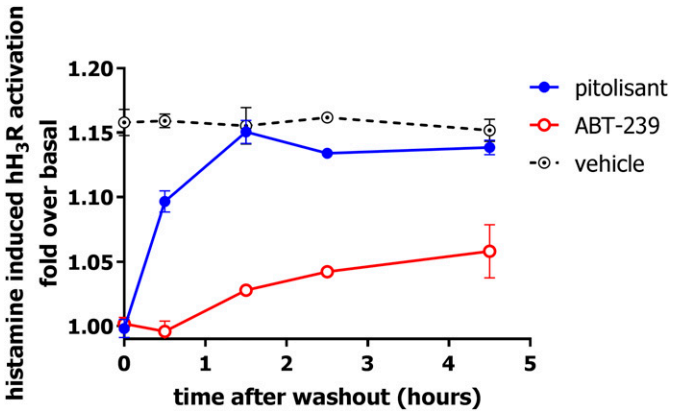

Fig. 6. Functional washout of 1 μM pitolisant or ABT-239 from the hH_3R and their ability to antagonize histamine-induced hH_3R activation. Cells were incubated overnight with either 1 μM pitolisant or ABT-239. Subsequently, cells were washed and allowed to re-equilibrate for different time periods before stimulation with histamine and detection of cAMP level using CAMYEL biosensor. Representative graph of three experiments performed in duplicate is shown.

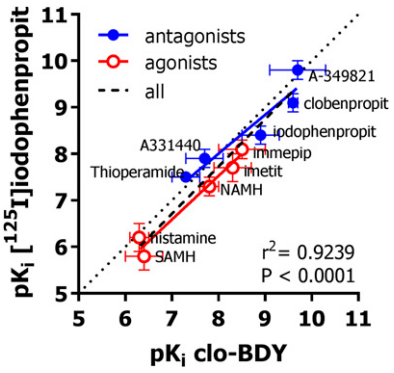

Fig. 7. Comparison of pK_i of unlabeled ligands for the hH_3R obtained from equilibrium NanoBRET assays with affinities obtained with [^{125}I]iodophenpropit from Bongers et al. (2007). Deming linear regression was used for data fitting. Dotted line shows line of unity.

concentrations (Bongers et al., 2007). Allosteric binding of sodium to GPCRs often reduces agonist affinity by stabilizing inactive receptor conformations but may also differently affect the binding of antagonists to the orthosteric binding site (Clark and Hill, 1995; Schnell and Seifert, 2010; Katritch et al., 2014; Wittmann et al., 2014; Newton et al., 2016; Hishinuma et al., 2017; Schiffmann and Gimpl, 2018). Nonetheless, most antagonists displayed affinities in the NanoBRET assay that were comparable to the radioligand-based competition-binding assay. Lower hH_4R-binding affinities for both agonist and antagonists were also observed in the NanoBRET-based binding assay on intact cells as compared with radioligand binding to cell homogenates, despite the fact that both labeled clo-BDY and [^{3}H]histamine are agonists on the hH_4R. Similar to the hH_3R, the presence of allosteric sodium in the NanoBRET buffer may reduce affinities of both agonists and antagonists for the hH_4R. In addition, competitive binding experiments and the Cheng-Prusoff equation assume reversible interaction between competing ligands and receptor. However, bound fluorescent agonists may induce receptor internalization during the course of a binding experiment on intact cells, which may result in the observation of lower pK_i values for unlabeled ligands as compared with binding assays on cell homogenates (Cheng and Prusoff, 1973; Guo et al., 2010).

The NanoBRET-based binding assay can detect binding of a fluorescent ligand to living cells expressing the Nluc-tagged receptor of interest with a high resolution in time, which also allows for the measurement of a full association-binding curve from a single sample (Hansen et al., 2017; Stoddart et al., 2018). Detection of the association binding of a fluorescent probe in the presence of unlabeled ligands allows quantification of the kinetic rate constants and K_D ($= k_{off}/k_{on}$) values of the latter. Since binding rate constants are sensitive to temperature, the ionic composition of buffer, and can be different in living cells versus cell homogenates or membrane preparations (Sykes et al., 2010; Vanderheyden and Benachour, 2017), one might anticipate that absolute rate constants of the few ligands that were previously reported in radioligand-binding studies might be different from those obtained using the current NanoBRET binding assay on living cells. Indeed, the hH_3R antagonist GSK1004723 displayed 5-fold faster dissociation kinetics in the NanoBRET binding assay compared to that previously reported (Slack et al., 2011), despite the lower temperature (25°C instead of 37°C) used in NanoBRET. In contrast, association and dissociation binding of the antagonist [^{3}H]A-349821 to membranes expressing the hH_3R revealed a 220-fold higher k_{on} value and similar k_{off} value as compared with the NanoBRET-based competition association assay (Witte et al., 2006).

Although a linear correlation was observed between pK_i and kinetic pK_D values of unlabeled hH_3R ligands in the NanoBRET-based binding assays, the kinetic pK_D values were consistently lower than the affinities that were obtained from the equilibrium binding assay. Hence, the absolute values of the determined binding rate constants in this competitive association binding should not be overinterpreted. However, evaluation of the functional recovery rate of hH_3R responsiveness to histamine stimulation upon dissociation of prebound long- and short-RT antagonists, under assay conditions comparable to the NanoBRET-based binding assay, revealed that obtained RT values are indeed very indicative of the duration of hH_3R antagonism of these antagonists.

Hitherto, only pitolisant (Wakix) is approved as an hH_3R-targeting antagonist to increase wakefulness and alertness in patients suffering from narcolepsy. Pitolisant was found to have a moderate RT (17 minutes) on the hH_3R, which consequently resulted in a relatively fast target recovery rate (Fig. 6). From the hH_3R antagonists that have been or are currently in clinical trials, bavisant and PF-03654746 have an RT comparable to pitolisant, whereas ABT-239 and GSK1004723 show substantially longer RTs. Recently, a new trial was initiated with bavisant to assess excessive daytime sleepiness in Parkinson's disease patients (NCT03194217). The long-residence-time antagonist GSK1004723 displayed a lack of in vivo efficacy, whereas ABT-239 failed to enter clinical trials due to drug safety issues (Hancock, 2006; Daley-Yates et al., 2012). Insomnia is frequently reported as a side effect of hH_3R antagonists in clinical trials, and hence long-RT ligands might further enhance this adverse event (Wijtmans et al., 2007; Brioni and Esbenshade, 2011; Sadek et al., 2016; Schwartzbach et al., 2017). Moreover, it was proposed that different ligands can address distinct hH_3R-related disorders (Esbenshade et al., 2006; Wijtmans et al., 2007; Sander et al., 2008). Therefore,

it remains to be seen what influence ligand kinetics have on the plethora of hH_3R-related therapeutic indications.

In conclusion, the NanoBRET-based competition equilibrium binding assay is a valuable tool to determine the binding parameters of unlabeled ligands for their receptors on living cells at reasonably high throughput under experimental conditions that better correspond to those used in functional assays, as compared with the traditional radioligand-binding studies on cell homogenates or isolated membranes.

Acknowledgments

Mouad El Mandili, Laura Bothof, and Rabia Asik are acknowledged for their help with Nluc-hH_3R and Nluc-hH_4R experiments, and Cas van der Horst is acknowledged for his help in radioligand displacement assays.

Authorship Contributions

Participated in research design: Mocking, Vischer, Leurs.

Conducted experiments: Mocking, Verweij.

Performed data analysis: Mocking, Verweij.

Wrote or contributed to the writing of the manuscript: Mocking, Vischer, Leurs.

References

Attali P, Gomeni R, Wersinger E, Poli S, and Venail F (2016) The effects of SENS-111, a new H4R antagonist, on vertigo induced by caloric test in healthy volunteers (HV) is related to plasma concentrations. *Clin Ther* **38**:e4.

Bongers G, Krueger KM, Miller TR, Baranowski JL, Estvander BR, Witte DG, Strakhova MI, van Meer P, Bakker RA, Cowart MD, et al. (2007) An 80-amino acid deletion in the third intracellular loop of a naturally occurring human histamine H3 isoform confers pharmacological differences and constitutive activity. *J Pharmacol Exp Ther* **323**:888–898.

Bosma R, Mocking TAM, Leurs R, and Vischer HF (2017) Ligand-binding kinetics on histamine receptors, in *Histamine Receptors as Drug Targets* (Tiligada E and Ennis M eds) pp 115–155, Springer New York, New York.

Brioni JD and Esbenshade T (2011) Discovery of histamine H3 antagonists for the treatment of cognitive disorders and Alzheimer's disease. *J Pharmacol Exp Ther* **336**:38–46.

Chabre M, Deterre P, and Antonny B (2009) The apparent cooperativity of some GPCRs does not necessarily imply dimerization. *Trends Pharmacol Sci* **30**:182–187.

Cheng Y and Prusoff WH (1973) Relation between the inhibiton constant (Ki) and the concentration of inhibitor which causes 50 percent inhibiton (IC50) of an enzymatic reaction. *Biochem Pharmacol* **22**:3099–3108.

Clark EA and Hill SJ (1995) Differential effect of sodium ions and guanine nucleotides on the binding of thioperamide and clobenpropit to histamine H3-receptors in rat cerebral cortical membranes. *Br J Pharmacol* **114**:357–362.

Copeland RA (2016) The drug-target residence time model: a 10-year retrospective. *Nat Rev Drug Discov* **15**:87–95.

Copeland RA, Pompliano DL, and Meek TD (2006) Drug-target residence time and its implications for lead optimization. *Nat Rev Drug Discov* **5**:730–739.

Daley-Yates P, Ambery C, Sweeney L, Watson J, Oliver A, and McQuade B (2012) The efficacy and tolerability of two novel H_1/H_3 receptor antagonists in seasonal allergic rhinitis. *Int Arch Allergy Immunol* **158**:84–98.

De Esch IJP, Gaffar A, Menge WMPB, and Timmerman H (1999) Synthesis and histamine H3 receptor activity of 4-(n-alkyl)-1H-imidazoles and 4-(ω-phenylalkyl)-1H-imidazoles. *Bioorg Med Chem* **7**:3003–3009.

Emami-Nemini A, Roux T, Leblay M, Bourrier E, Lamarque L, Trinquet E, and Lohse MJ (2013) Time-resolved fluorescence ligand binding for G protein-coupled receptors. *Nat Protoc* **8**:1307–1320.

Goldman LA, Cutrone E, Kotenko S, Krause C, and Langer J (1996) Modification of vectors pEF-BOS, pcDNA1 and pcDNA3 result in improved convenience and expression. *Biotechniques* **21**:1013–1015.

Guo D, Dijksteel GS, Van Duijl T, Heezen M, Heitman LH, and IJzerman AP (2016) Equilibrium and kinetic selectivity profiling on the human adenosine receptors. *Biochem Pharmacol* **105**:34–41.

Guo N, Guo W, Kralikova M, Jiang M, Schieren I, Narendran R, Slifstein M, Abi-Dargham A, Laruelle M, Javitch JA, et al. (2010) Impact of D2 receptor internalization on binding affinity of neuroimaging radiotracers. *Neuropsychopharmacology* **35**:806–817.

Hancock AA (2006) The challenge of drug discovery of a GPCR target: analysis of preclinical pharmacology of histamine H3 antagonists/inverse agonists. *Biochem Pharmacol* **71**:1103–1113.

Hansen AH, Sergeev E, Pandey SK, Hudson BD, Christiansen E, Milligan G, and Ulven T (2017) Development and characterization of a fluorescent tracer for the free fatty acid receptor 2 (FFA2/GPR43). *J Med Chem* **60**:5638–5645.

Hishinuma S, Kosaka K, Akatsu C, Uesawa Y, Fukui H, and Shoji M (2017) Asp73-dependent and -independent regulation of the affinity of ligands for human histamine H1receptors by Na+. *Biochem Pharmacol* **128**:46–54.

Hoffmann C, Castro M, Rinken A, Leurs R, Hill SJ, and Vischer HF (2015) Ligand residence time at G-protein–coupled receptors—why we should take our time to study it. *Mol Pharmacol* **88**:552–560.

Jablonowski JA, Grice CA, Chai W, Dvorak CA, Venable JD, Kwok AK, Ly KS, Wei J, Baker SM, Desai PJ, et al. (2003) The first potent and selective non-imidazole human histamine H4 receptor antagonists. *J Med Chem* **46**:3957–3960.

Jansen FP, Wu TS, Voss H-P, Steinbusch HWM, Vollinga RC, Rademaker B, Bast A, and Timmerman H (1994) Characterization of the binding of the first selective radiolabeled histamine H3-receptor antagonist, [125I]-iodophenpropit, to rat brain. *Br J Pharmacol* **113**:355–362.

Katritch V, Fenalti G, Abola EE, Roth BL, Cherezov V, and Stevens RC (2014) Allosteric sodium in class A GPCR signaling. *Trends Biochem Sci* **39**:233–244.

Kollb-Sielecka M, Demolis P, Emmerich J, Markey G, Salmonson T, and Haas M (2017) The European Medicines Agency review of pitolisant for treatment of narcolepsy: summary of the scientific assessment by the Committee for Medicinal Products for Human Use. *Sleep Med* **33**:125–129.

Ligneau X, Perrin D, Landais L, Camelin J-C, Calmels TPG, Berrebi-Bertrand I, Lecomte J-M, Parmentier R, Anaclet C, Lin J-S, et al. (2007) BF2.649 [1-{3-[3-(4-Chlorophenyl)propoxy]propyl}piperidine, hydrochloride], a nonimidazole inverse agonist/antagonist at the human histamine H3 receptor: preclinical pharmacology. *J Pharmacol Exp Ther* **320**:365–375.

Lim HD, Istyastono EP, van de Stolpe A, Romeo G, Gobbi S, Schepers M, Lahaye R, Menge WMBP, Zuiderveld OP, Jongejan A, et al. (2009) Clobenpropit analogs as dual activity ligands for the histamine H3 and H4 receptors: synthesis, pharmacological evaluation, and cross-target QSAR studies. *Bioorg Med Chem* **17**:3987–3994.

Lim HD, Smits RA, Bakker RA, van Dam CME, de Esch IJP, and Leurs R (2006) Discovery of S -(2-Guanidylethyl)-isothiourea (VUF 8430) as a potent nonimidazole histamine H 4 receptor agonist. *J Med Chem* **49**:6650–6651.

Lim HD, van Rijn RM, Ling P, Bakker R, Thurmond RL, and Leurs R (2005) Evaluation of histamine H1-, H2-, and H3-receptor ligands at the human histamine H4 receptor: identification of 4-methylhistamine as the first potent and selective H4 receptor agonist. *J Pharmacol Exp Ther* **314**:1310–1321.

Lovenberg TW, Roland BL, Wilson SJ, Jiang X, Pyati J, Huvar A, Jackson MR, and Erlander MG (1999) Cloning and functional expression of the human histamine H3 receptor. *Mol Pharmacol* **55**:1101–1107.

Mirzahosseini A, Kovács M, Kánai K, Csutora P, and Dalmadi B (2015) BODIPY®FL histamine as a new modality for quantitative detection of histamine receptor upregulation upon IgE sensitization in murine bone marrow-derived mast cells. *Cytometry A* **87**:23–31.

Motulsky HJ and Mahan LC (1984) The kinetics of competitive radioligand binding predicted by the law of mass action. *Mol Pharmacol* **25**:1–9.

Newton CL, Wood MD, and Strange PG (2016) Examining the effects of sodium ions on the binding of antagonists to dopamine D2 and D3 receptors. *PLoS One* **11**:e0158808.

Nijmeijer S, Engelhardt H, Schultes S, Van De Stolpe C, Lusink V, De Graaf C, Wijtmans M, Haaksma EEJ, De Esch IJP, Stachurski K, et al. (2013a) Design and pharmacological characterization of VUF14480, a covalent partial agonist that interacts with cysteine 983.36 of the human histamine H4 receptor. *Br J Pharmacol* **170**:89–100.

Nijmeijer S, Vischer HF, Sirci F, Schultes S, Engelhardt H, de Graaf C, Rosethorne EM, Charlton SJ, and Leurs R (2013b) Detailed analysis of biased histamine H4 receptor signalling by JNJ 7777120 analogues. *Br J Pharmacol* **170**:78–88.

Novak N, Mete N, Bussmann C, Maintz L, Bieber T, Akdis M, Zumkehr J, Jutel M, and Akdis C (2012) Early suppression of basophil activation during allergen-specific immunotherapy by histamine receptor 2. *J Allergy Clin Immunol* **130**:1153–1158.e2.

Panula P, Chazot PL, Cowart M, Gutzmer R, Leurs R, Liu WLS, Stark H, Thurmond RL, and Haas HL (2015) International union of basic and clinical pharmacology. XCVIII. Histamine receptors. *Pharmacol Rev* **67**:601–655.

Sadek B, Łażewska D, Hagenow S, Kieć-Kononowicz K, and Stark H (2016) Histamine H3R antagonists: from scaffold hopping to clinical candidates, in *Histamine Receptors: Preclinical and Clinical Aspects* (Blandina P and Passani MB eds) pp 109–155, Springer International Publishing, Cham, Switzerland.

Sander K, Kottke T, and Stark H (2008) Histamine H3 receptor antagonists go to clinics. *Biol Pharm Bull* **31**:2163–2181.

Schiffmann A and Gimpl G (2018) Sodium functions as a negative allosteric modulator of the oxytocin receptor. *Biochim Biophys Acta Biomembr* **1860**:1301–1308.

Schnell D and Seifert R (2010) Modulation of histamine H3 receptor function by monovalent ions. *Neurosci Lett* **472**:114–118.

Scholten DJ, Canals M, Wijtmans M, De Munnik S, Nguyen P, Verzijl D, De Esch IJP, Vischer HF, Smit MJ, and Leurs R (2012) Pharmacological characterization of a small-molecule agonist for the chemokine receptor CXCR3. *Br J Pharmacol* **166**:898–911.

Schwartzbach CJ, Grove RA, Brown R, Tompson D, Then Bergh F, and Arnold DL (2017) Lesion remyelinating activity of GSK239512 versus placebo in patients with relapsing-remitting multiple sclerosis: a randomised, single-blind, phase II study. *J Neurol* **264**:304–315.

Slack RJ, Russell LJ, Hall D, Luttmann M, Ford J, Saunders K, Hodgson ST, Connor HE, Browning C, and Clark KL (2011) Pharmacological characterization of GSK1004723, a novel, long-acting antagonist at histamine H 1 and H 3 receptors. *Br J Pharmacol* **164**:1627–1641.

Smits RA, de Esch IJP, Zuiderveld OP, Broeker J, Sansuk K, Guaita E, Coruzzi G, Adami M, Haaksma E, and Leurs R (2008) Discovery of quinazolines as histamine H 4 receptor inverse agonists using a scaffold hopping approach. *J Med Chem* **51**:7855–7865.

Soave M, Stoddart LA, Brown A, Woolard J, and Hill SJ (2016) Use of a new proximity assay (NanoBRET) to investigate the ligand-binding characteristics of three fluorescent ligands to the human β1-adrenoceptor expressed in HEK-293 cells. *Pharmacol Res Perspect* **4**:e00250.

Stoddart LA, Johnstone EKM, Wheal AJ, Goulding J, Robers MB, Machleidt T, Wood KV, Hill SJ, and Pfleger KDG (2015) Application of BRET to monitor ligand binding to GPCRs. *Nat Methods* **12**:661–663.

Stoddart LA, Kilpatrick LE, and Hill SJ (2018a) NanoBRET approaches to study ligand binding to GPCRs and RTKs. *Trends Pharmacol Sci* **39**:136–147.

Stoddart LA, Vernall AJ, Bouzo-Lorenzo M, Bosma R, Kooistra AJ, de Graaf C, Vischer HF, Leurs R, Briddon SJ, Kellam B, et al. (2018b) Development of novel

fluorescent histamine H1-receptor antagonists to study ligand-binding kinetics in living cells. *Sci Rep* **8**:1572.
Strange PG (2008) Agonist binding, agonist affinity and agonist efficacy at G protein-coupled receptors. *Br J Pharmacol* **153**:1353–1363.
Sykes DA, Dowling MR, and Charlton SJ (2009) Exploring the mechanism of agonist efficacy: a relationship between efficacy and agonist dissociation rate at the muscarinic M3 receptor. *Mol Pharmacol* **76**:543–551.
Sykes DA, Dowling MR, and Charlton SJ (2010) Measuring receptor target coverage: a radioligand competition binding protocol for assessing the association and dissociation rates of unlabeled compounds. *Curr Protoc Pharmacol* **Chapter 9**:unit 9.14.
Sykes DA, Moore H, Stott L, Holliday N, Javitch JA, Lane JR, and Charlton SJ (2017) Extrapyramidal side effects of antipsychotics are linked to their association kinetics at dopamine D2 receptors. *Nat Commun* **8**:763.
Thurmond RL (2015) The histamine H4 receptor: from orphan to the clinic. *Front Pharmacol* **6**:65.
Thurmond RL, Venable J, Savall B, La D, Snook S, Dunford PJ, and Edwards JP (2017) Clinical development of histamine H4 receptor antagonists, in *Histamine and Histamine Receptors in Health and Disease* (Hattori Y and Seifert R eds) pp 301–320, Springer International Publishing, Cham, Switzerland.
Tomasch M, Schwed JS, Paulke A, and Stark H (2012) Bodilisant-a novel fluorescent, highly affine histamine H3 receptor ligand. *ACS Med Chem Lett* **4**:269–273.
van der Goot H, Schepers M, Sterk G, and Timmerman H (1992) Isothiourea analogues of histamine as potent agonists or antagonists of the histamine H3-receptor. *Eur J Med Chem* **27**:511–517.
Vanderheyden PML and Benachour N (2017) Influence of the cellular environment on ligand binding kinetics at membrane-bound targets. *Bioorg Med Chem Lett* **27**:3621–3628.
Vauquelin G, Van Liefde I, and Swinney DC (2015) Radioligand binding to intact cells as a tool for extended drug screening in a representative physiological context. *Drug Discov Today Technol* **17**:28–34.
Vernall AJ, Hill SJ, and Kellam B (2014) The evolving small-molecule fluorescent-conjugate toolbox for Class A GPCRs. *Br J Pharmacol* **171**:1073–1084.
Verweij EWE, Leurs R, and Vischer HF (2017) Methods to study the molecular pharmacology of the histamine H4 receptor, in *Histamine Receptors as Drug Targets* (Tiligada EEM ed) pp 157–181, Humana Press, New York.
Vollinga RC, de Koning JP, Jansen FP, Leurs R, Menge WMPB, and Timmerman H (1994) A new potent and selective histamine H3 receptor agonist, 4-(1H-imidazol-4-ylmethyl)piperidine. *J Med Chem* **37**:332–333.
Vollinga RC, Menge WMPB, Leurs R, and Timmerman H (1995) Homologs of histamine as histamine H3 receptor antagonists: a new potent and selective H3 antagonist, 4(5)-(5-aminopentyl)-1H-imidazole. *J Med Chem* **38**:266–271.
Wijtmans M, Leurs R, and de Esch I (2007) Histamine H3 receptor ligands break ground in a remarkable plethora of therapeutic areas. *Expert Opin Investig Drugs* **16**:967–985.
Witte DG, Yao BB, Miller TR, Carr TL, Cassar S, Sharma R, Faghih R, Surber BW, Esbenshade T, Hancock A, et al. (2006) Detection of multiple H3 receptor affinity states utilizing [3H]A-349821, a novel, selective, non-imidazole histamine H3 receptor inverse agonist radioligand. *Br J Pharmacol* **148**:657–670.
Wittmann H-J, Seifert R, and Strasser A (2014) Mathematical analysis of the sodium sensitivity of the human histamine H3 receptor. *In Silico Pharmacol* **2**:1.
Zwier JM, Roux T, Cottet M, Durroux T, Douzon S, Bdioui S, Gregor N, Bourrier E, Oueslati N, Nicolas L, et al. (2010) A fluorescent ligand-binding alternative using tag-lite® technology. *J Biomol Screen* **15**:1248–1259.

Address correspondence to: Rob Leurs, Vrije Universiteit Amsterdam, Faculty of Science, Division of Medicinal Chemistry, O|2 building, De Boelelaan 1108, 1081 HZ Amsterdam, The Netherlands. E-mail: r.leurs@vu.nl